Preliminary Communication

For reprint orders, please contact: reprints@futuremedicine.com

Nanomedicine

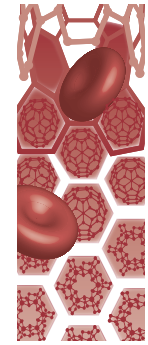

Monitoring nanoparticle-mediated cellular hyperthermia with a high-sensitivity biosensor

Amarnath Mukherjee[1], Mark Castanares[†,1], Mohammad Hedayati[2], Michele Wabler[2], Bruce Trock[1], Prakash Kulkarni[1], Ronald Rodriguez[1,§], Robert H Getzenberg[¶,1], Theodore L DeWeese[2], Robert Ivkov[‡,*,2] & Shawn E Lupold[‡,*,1,2]

[1]The James Buchanan Brady Urological Institute & Department of Urology, Johns Hopkins Medical Institutions, Baltimore, MD, USA

[2]Department of Radiation Oncology, Johns Hopkins Medical Institutions, Baltimore, MD, USA

*Authors for correspondence:
Tel.: +1 410 502 4822
Fax: +1 410 502 1853
slupold@jhmi.edu
Tel.: +1 443 287 7282
Fax: +1 410 502 2821
rivkov1@jhmi.edu

[‡]Authors contributed equally

[†]Current affiliation: Eli Lilly & Company, Indianapolis, IN, USA

[§]Current affiliation: University of Texas Health Science Center San Antonio, TX, USA

[¶]Current affiliation: GTx, Inc., Memphis, TN, USA

Aim: To develop and apply a heat-responsive and secreted reporter assay for comparing cellular response to nanoparticle (NP)- and macroscopic-mediated sublethal hyperthermia. **Materials & methods:** Reporter cells were heated by water bath (macroscopic heating) or iron oxide NPs activated by alternating magnetic fields (nanoscopic heating). Cellular responses to these thermal stresses were measured in the conditioned media by secreted luciferase assay. **Results & conclusion:** Reporter activity was responsive to macroscopic and nanoparticle heating and activity correlated with measured macroscopic thermal dose. Significant cellular responses were observed with NP heating under doses that were insufficient to measurably change the temperature of the system. Under these conditions, the reporter response correlated with proximity to cells loaded with heated nanoparticles. These results suggest that NP and macroscopic hyperthermia may be distinctive under conditions of mild hyperthermia.

Original submitted 10 May 2013; Revised submitted 31 October 2013

Keywords: heat shock • hyperthermia • iron oxide nanoparticle • *Metridia* luciferase • nanoparticle

Advances in nanotechnology that create nanoparticles (NPs) capable of generating localized heat offer the potential to reshape the concept of targeted and focal hyperthermia as a cancer therapy [1–3]. In 1979, Gordon *et al.* first described the use of intracellular magnetic particles to generate hyperthermia in a rat mammary tumor model [4]. Today, several iron- and gold-based NPs are undergoing preclinical and clinical evaluation for hyperthermia in various cancers [5–8]. Despite the rapid advance of these technologies, a number of questions remain unanswered regarding the mechanism of heat transfer from NP-mediated hyperthermia to cells and tissues. Characterizing the nature of NP heating and its relationship to macroscopic hyperthermia continues to present a significant challenge.

It is generally accepted that exposing mammalian cells to elevated temperatures produces profound and varied dose-dependent consequences. Thermal exposure or dose is typically defined as exposure 'time at temperature' because both temperature and exposure time at a specific temperature produce different responses [9]. Heat is a mechanical incoherent energy that indiscriminately affects a cell at the molecular level. Mammalian cells are sensitive to thermal fluctuations, requiring a narrow range of environmental temperature to maintain homeostasis. When the temperature deviates outside this range, multiple cellular processes are potentially compromised or damaged, placing cells in distress. Cells respond by invoking various survival, maintenance and repair processes as part of general coping mechanisms to limit or repair damage [10].

It is this general sensitivity of mammalian cells to heat that has motivated exploration of hyperthermia for cancer therapy. Early

Future Medicine part of fsg

efforts to quantify cellular response to hyperthermia with clinical intent were based upon measurements of the surviving fraction of populations of cells that were exposed to varying thermal doses [9]. Using these survival end points, studies of heated cultured human cells typically show a significant decrease in survival (i.e., 'break-point') at 42.5–43.0°C, leading to a generally accepted cytotoxic temperature criterion of 43°C. This cytotoxic temperature threshold has been generally confirmed in clinical studies, leading to its acceptance as a dose-metric standard for biological and clinically relevant hyperthermia. It is worth emphasizing, however, that the basis of this accepted dose metric is empirical measurements of the surviving fraction of a cell population following exposure to thermal stress, and normalized relative to an unexposed control sample. The effects on cells exposed to sublethal thermal doses (i.e., temperature <43°C) has also been studied, but presents unique challenges for characterization and has been considered less clinically relevant, until recently [11,12].

It has been suggested that cell exposure to low-level (i.e., sublethal) thermal stress induces potentially lethal lesions that may be repaired given sufficient time, provided the repair processes are intact [11]. Recently published results suggest that when assayed by end points other than survival, human (cancer) cells demonstrate profound sensitivity to temperatures and thermal doses well below 'cytotoxic' levels established from survival-only end points. Krawczyk *et al.* report that human cancer cells demonstrate sensitivity to mild elevation in temperatures such as 41°C [12]. In a series of experiments, they report that mild and sublethal hyperthermia initiates rapid (within ~15 min) and lasting (>3 h) degradation of BRCA2, leading to compromised or abrogated DNA double-strand break repair. During this time, cells are vulnerable to ionizing radiation, as demonstrated by decreased survival following exposure to radiation. If, on the other hand, another (potentially) cytotoxic agent such as radiation is avoided during a 'repair window', affected cells will eventually return to the native state without significant cell death. In a separate study, Kariya *et al.* performed gene expression analysis to identify 114 different transcripts that were consistently activated by mild and nonlethal hyperthermia at 41°C for 30 min [10]. Responsive genes were involved in pathways of cellular growth and maintenance and each gene had differential expression and kinetic patterns. Thus, nonlethal hyperthermia can induce a complex series of molecular and cellular responses, which could be applied as sensitive end points for the study of mild hyperthermia.

Choice of end point may be only one consideration that influences the interpretation of outcome when exposing human cells to thermal doses. Some recent reports suggest that cells may be sensitive to the nature of the heating agent itself when they are exposed to sublethal (in the classical sense) or lethal thermal doses. For example, Creixell *et al.* reported that EGF receptor-targeted hyperthermia with magnetic NPs induced cell death without a measurable temperature change [13]. Similar results have also been reported by Asin *et al.* and Villanueva *et al.* [14,15]. NP-mediated hyperthermia can also cause cellular damage and stress without affecting cellular viability [16]. Other cell survival-based studies of NP versus water bath-mediated hyperthermia have observed differential responses at identical thermal doses [17,18]. Thus it would seem that NP-mediated hyperthermia may perturb cellular systems by mechanisms that are distinct from macroscopic hyperthermia, although this suggestion is potentially controversial. More detailed studies of NP heating and cellular responses to sublethal thermal stress may provide new insights into the biology of NP-mediated hyperthermia.

Several methods have been developed to evaluate heating at cellular or subcellular length scales. Fluorescent-based probes can be used to characterize changes in the temperature of the cellular environment through quantifiable changes in fluorescent properties [19–21]. Similarly, temperature can influence the structure of fluorescent and bioluminescent proteins, such as luciferase, to provide a quantifiable loss of signal that correlates with increases in temperature [22]. Perhaps more relevant and informative are reporters of cellular response or alterations in cellular processes when perturbed by changes in temperature. Such reporter systems are inherently designed to measure the thermal stress response rather than temperature directly. Transcriptional reporters that are activated by cellular heat shock pathways can be applied to quantify cellular responses to thermal stress. For example, the *HSP70* promoter, when driving the expression of the firefly luciferase reporter gene, can detect thermal stress to cells and tissues both *ex vivo* and *in vivo* [23]. The development and application of such systems may provide a useful tool to assess cellular responses to sublethal thermal doses by different heating sources.

Here we report the development and initial findings from the application of a sensitive transcriptional reporter system to measure cellular response following NP and water bath heating. The heat shock element (HSE), a genetic enhancer sequence that is present in the *HSP70* gene and contributes to cellular heat response, was used to regulate the expression of a constitutively secreted bioluminescent reporter, *Metridia* luciferase (MLuc) [24–26]. The expressed reporter can be conveniently collected from media

providing a nondestructive assay to measure thermal response. The secreted reporter also enabled reproducible assays by avoiding confounding absorbance from iron oxide NPs. When cells were exposed to varying heat doses in a water bath, which was used to 'calibrate' response, the relative secreted bioluminescent signal directly corresponded to both temperature and thermal dose (i.e., time at temperature for each individual treatment temperature). The linear response range was restricted to low thermal doses 40–43°C, presumably because dying cells ceased secretion of the reporter. Results of water bath heating were compared with NP-mediated hyperthermia. Notably, the biological sensor was still activated when cells were exposed to lower NP-mediated thermal doses, measured by single-point thermometry for which there was no measurable macroscopic temperature change. Using this model, we investigated cellular responses to NP hyperthermia from within the cells and from adjacent cells loaded with NPs under various thermal doses. We hypothesize from these preliminary studies that cells may be sensitive to transient and nonlethal heat transfer produced by NP heating within or adjacent to the cell.

Materials & methods

Nanoparticle & chemicals

Bionized nanoferrite (BNF) particles coated with hydroxymethyl starch, having a mean hydrodynamic diameter of 100 nm, were purchased from micromod Partikeltechnologie, GmbH (Rostock, Germany). Lipofectamine™ 2000 and optiMEM were purchased from Life Technologies (CA, USA). All restriction enzymes were purchased from New England Biolabs Inc. (MA, USA). All other reagents/chemicals were bought from Sigma-Aldrich (MO, USA) unless mentioned otherwise.

Cell culture

HCT-116 cells were purchased from ATCC (VA, USA) and cultured under recommended conditions. Briefly, cells were cultured in McCoy's 5A medium (Mediatech, Inc., VA, USA) containing 10% fetal bovine serum (Sigma Chemical Co., MO, USA) and 1% ciprofloxacin at 37°C in a humidified atmosphere of 5% CO_2 in air. Cultures of 85–90% confluency were used for all experiments. Screens for mycoplasma contamination were performed regularly.

Plasmid construction

The translucent HSE luciferase vector that contains a minimal TK promoter and three repeats of a 15-bp HSE of sequence CTGGAATTTTCTAGA was graciously provided by Dr Martin Gleeve (University of British Columbia, BC, Canada). The humanized MLuc cDNA was obtained from a pDonor-hb-actin-MLuc plasmid through double digestion with NcoI and HpaI and subcloned into the HSE luciferase vector, ultimately replacing firefly luciferase to generate pHSE–MLuc. The control plasmid (cntrl-MLuc) was generated by deleting the HSE sequence by digestion with NheI and BglII restriction enzymes followed by blunt end ligation after treatment by Klenow fragment. The integrity of the resulting cntrl-MLuc and pHSE–MLuc were confirmed by diagnostic restriction mapping and functional assays.

Plasmid transfection

Cells were counted and plated in T75 flasks 1 day prior to transfection. A total of 25 µg of pHSE–MLuc (or control) DNA (diluted to 1.5 ml with optiMEM) were mixed with 60 µl of Lipofectamine 2000 (diluted to 1.5 ml with optiMEM) for 15–20 min as recommended by the manufacturer. A total of 12 ml of RPMI containing 10% fetal bovine serum was added to the resulting lipoplexes, which were then added to cells. After addition, the cells were incubated in a humidified atmosphere containing 5% CO_2 at 37°C.

NP loading into cells

NPs were loaded into cells as previously described [27]. Briefly, variable concentrations of 100 nm BNF particles and sterile poly-D-lysine (Sigma-Aldrich; Supplementary Table 1, see online at www.futuremedicine.com/doi/suppl/nmm.13.207) were added to the medium of cultured HCT-116 cells and incubated for 12–16 h. Extracellular particles were removed by three rinses with Dulbecco's phosphate-buffered saline. Cells were detached using a cell scraper and resuspended into the required amount of media.

Cell pellet formation & alternating magnetic field exposure

After loading the HCT-116 cells with reporter and NPs as described above, approximately 1 million detached cells were centrifuged at 1000 rpm for 5 min to form cell pellets. All pellets were prepared in duplicate and maintained in a constant volume of 1 ml of culture media in a 5-ml tube, both before and during treatment. Samples were then placed in the center of a four-turn solenoid, which was lined with a circulating water jacket. The water jacket was maintained at 37°C, and all samples were allowed to equilibrate within 2–3°C. The alternating magnetic field (AMF) system has previously been described [28]. Briefly, the AMF system comprised three main components: a power supply, an external impedance matching network and a solenoid coil. The power supply is an 80-kW induction heat-

ing system manufactured by PPECO (CA, USA) that provides an alternating current to a resonant circuit with variable frequencies (135–440 kHz). The external impedance match network (AMF Life Systems, Inc., MI, USA) was adjusted for stable oscillation at 150 ± 1 kHz. The four-turn solenoid coil had an inner diameter of 45.5 mm and was constructed from dehydrated annealed soft-copper refrigerator tubing having a 6.4-mm outer diameter. Within the solenoid, a polypropylene jacket, through which distilled water was circulated, provided a thermal barrier to heat generated directly by the solenoid. For all cell-heating experiments, the AMF amplitude was fixed at 80 kA/m and cells (at a density of ~10^6 cells/ml of media and then centrifuged to form a pellet) were exposed for 20 min. The magnitude of the magnetic field was measured prior to cell exposure at the center of the solenoid using a magnetic field probe. For each cell pellet exposed to AMF, a control-matched pellet having same cells was separately maintained following similar conditions.

Thermometry

The surface temperature of the pellet was measured during AMF exposure by placing calibrated radiofrequency-resistant fiber-optic temperature probes (FISO Technologies, Quebec City, Canada) on the pellet surface. Temperature data were recorded at 1-s intervals for the entire treatment time.

Bioluminescent reporter assay

After treatment (AMF, water bath or PCR heat block) the exposed and nonexposed HCT-116 cells were seeded onto a 96-well plate with a cell density of 50,000 cells/well. After the desired time (24 h unless otherwise mentioned), 80 µl of conditioned media was transferred to nonsterile white bottom 96-well luminometer plates (BD Biosciences, MA, USA). For non-end point time course assays, cells received new media at each time point after conditioned media harvest. Using a Microbeta Wallac (Perkin-Elmer, MA, USA), 100 µl Renilla buffer (1.1 M NaCl, 220 mM K_xPO_4, 1.3 mM NaN_3, 2.2 mM NA_2 EDTA and 0.44 mg/ml bovine serum albumin) containing the MLuc substrate, coelenterazine (1.43 mM) was injected into each well and luminescence was measured for 10 s. Data were plotted over time as fold (ratio) arbitrary light units relative to control cohorts.

MTS assay for cell viability

After the removal of media for the MLuc assay, 100 µl of fresh media were added to the cells in the 96-well plate. Cell viability was quantified 2–4 h later by MTS (Promega Corporation, WI, USA) and absorbance at 550 nm according to the manufacturer's protocol.

Inductively coupled plasma mass spectroscopy

Subsequent to treatment, a portion (~5 × 10^5) of the cell preparation was again pelleted by centrifugation and stored at -20°C for further characterization by inductively coupled plasma mass spectroscopy (ICP-MS). These samples were suspended in nitric acid and thermally digested using a two-stage ramp-to-temperature microwave method. A MARS5 Xpress microwave (CEM Corporation, NC, USA) was used. Digested samples were diluted for mass spectrometric evaluation and the total iron content of the samples was determined using an Agilent 7500ce ICP-MS (Agilent Technologies, CA, USA). An eight-point calibration curve was performed prior to sample analysis. The total iron content per cell was calculated, accounting for the number of cells provided.

Statistical analysis

Data were expressed as mean ± standard deviation and statistically analyzed by the two-tailed unpaired Student t-test using Microsoft Excel software program (Microsoft, WA, USA). Data were primarily considered significant if $p < 0.001$. To calculate the inflection temperature, the Join Point Regression software from National Cancer Institute was used [29]. Assay linearity was determined by linear regression analysis.

Results

Concept & generation of a biologic sensor

The HSE is a genetic enhancer that is present in the *HSP70* gene and contributes to cellular heat response [25,26]. Here, we used this element within a bioluminescent reporter construct to detect cellular response to thermal stress by enhanced activation of the constitutively active minimal herpes simplex virus thymidine kinase promoter. To circumvent the influence of NP components on the bioluminescent or chemical properties of the reporter assay, a secreted bioluminescent reporter was applied [24]. In this way, the reporter assay can be performed with cellular supernatant in the absence of cellular or NP components. This is particularly important because iron oxide NPs strongly absorb light over a broad range of the visible spectrum. Because reporter activity is measured in the cellular media, activity can be continually measured from a single sample. The cells were then available for final *in situ* tests of biologic responses, such as cell viability.

Characterization of the biologic sensor with macroscopic heating

Heat-induced overexpression of the biologic reporter

We first used water bath-mediated heating to characterize the response of the HSE–MLuc reporter system,

prior to its application to NP-mediated heating studies. For all studies, HCT-116 colon cancer cells were applied as a cell-line model. The cells were transiently transfected with either the HSE–MLuc reporter plasmid or a negative control MLuc plasmid that lacked the HSE element. Transfected cells were then equally distributed into independent cohorts for comparative heating studies (Figure 1, top). With this method, the relative response to heat was measured in samples of cells arising from the same transfected batch, thus ensuring identical (within statistical and individual cell variation) plasmid content among the samples. It is also worth noting that such a 'normalization' does not provide adequate control to compare among samples prepared from different transfection batches, unless one applies an independent method for measuring and normalizing transfection efficiency. One day following transfection, the matched cell groups were either heated (42°C for 30 min) or maintained at physiological temperature (37°C). After heat shock, the treated cells were then immediately transferred to multiwell plates and fresh media was provided for standard growth conditions. The secreted MLuc activity was then measured from the media at 0, 4 and 24 h after water-bath hyperthermia treatment and reported as relative light units (RLU). Heat-induced increases in secreted MLuc activity were observed from the cell media as soon as 4 h after exposure to hyperthermia (Figure 2A). There was no detectable thermal-induced-expression of MLuc in cells transfected with the negative control reporter that lacks the HSE element (Figure 2B). HSE–MLuc reporter signal continues to accumulate 24 h after treatment. This 24-h time point was selected for media harvest for all of the following heating studies. It should be noted that choice of a single time point for collection of reporter ensures sufficient signal intensity to enable quantitative assay results. On the other hand, a 24-h assay point provides limited time-dependent (kinetic) response information. It is by nature, a measure of cumulative response and signal integrated over the 24-h period following exposure.

Dose response & sensitivity of the reporter

The response of a cell to elevated temperatures is a reaction to both temperature and exposure time at

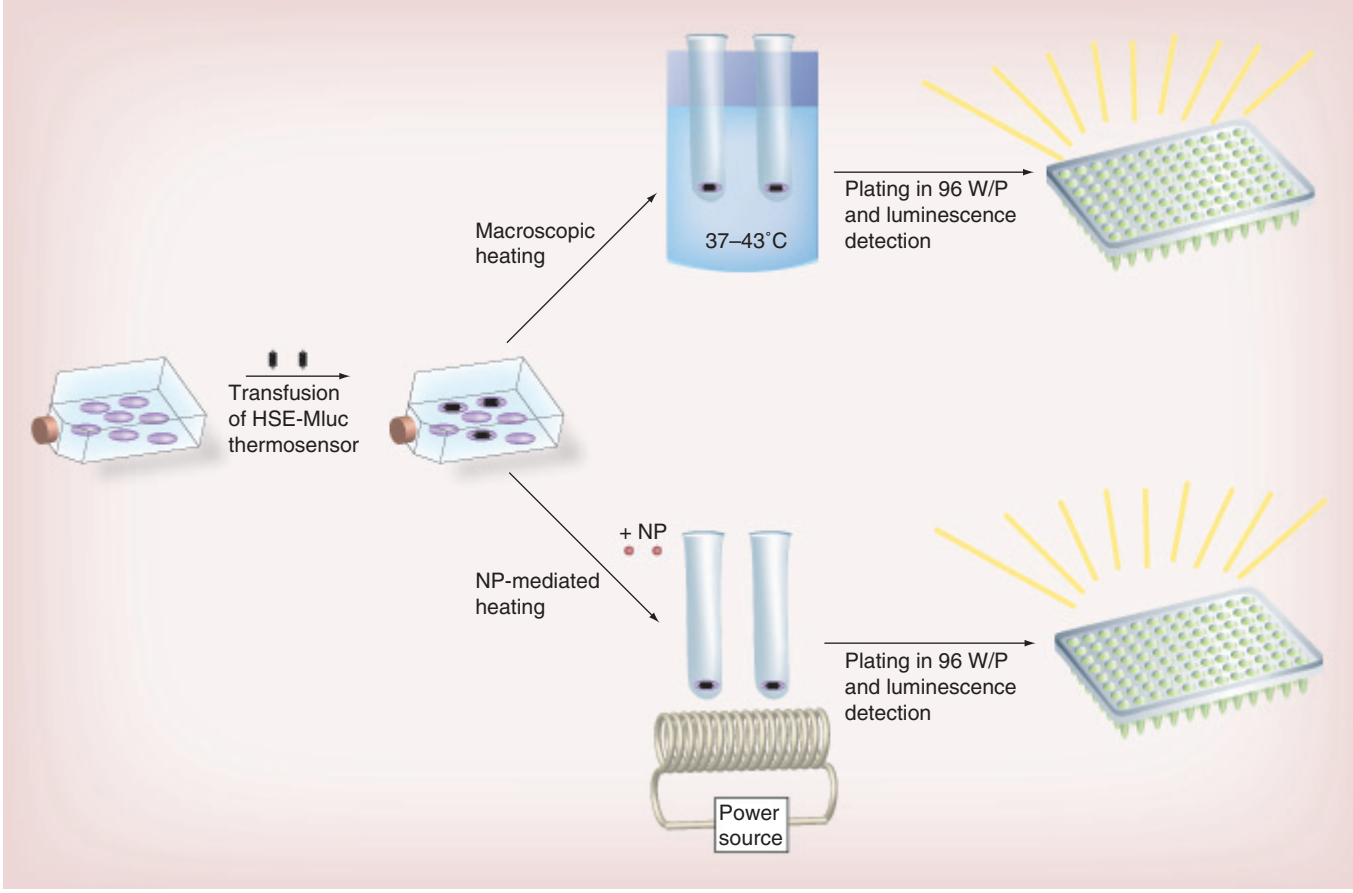

Figure 1. Schematic of heat responsive reporter loading, cell treatment and reporter detection.
HSE: Heat shock element; MLuc: *Metridia* luciferase; NP: Nanoparticle; W/P: Well plate.

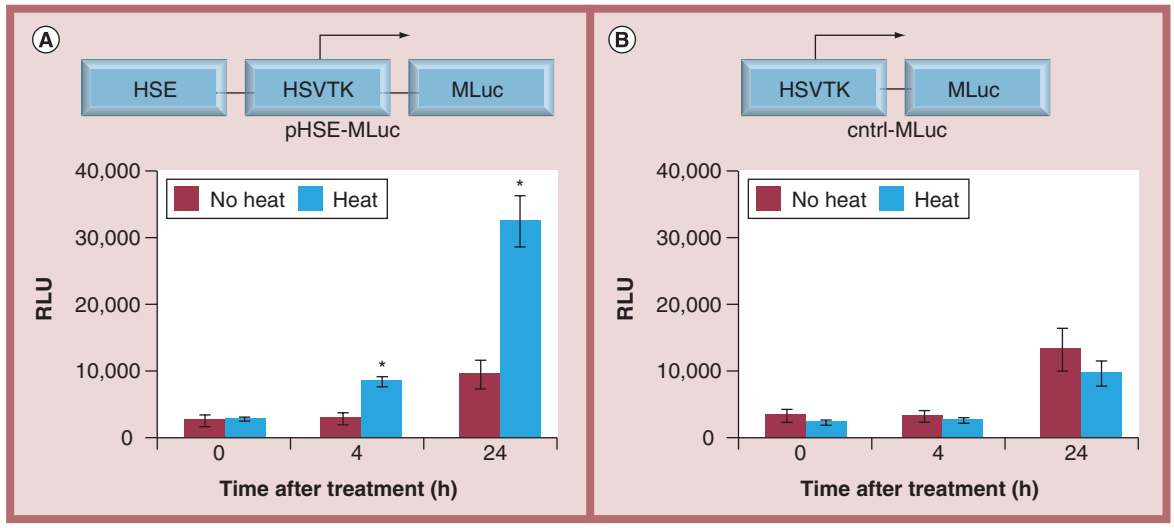

Figure 2. Reporter characterization following a single thermal dose. (A) Heat-induces activation of HSE–MLuc plasmid. Cells were transfected with pHSE–MLuc plasmid and heated by water bath at 42°C for 30 min or kept unheated. The cells were plated and media was collected at indicated time points and subjected to MLuc assay. Reporter schematic is indicated for pHSE–MLuc and cntrl-MLuc plasmids. **(B)** Heat does not activate the cntrl-MLuc plasmid. Cells were transfected with cntrl-MLuc plasmid and heated at 42°C for 30 min or kept unheated. The cells were plated and media was collected at indicated time points and subjected to MLuc assay. Results are reported as RLU.

*Statistical significance ($p < 0.001$) relative to nonheated samples as determined by Student's t-test. Error bars represent standard deviation of four independent measurements.

cntrl: Control; HSE: Heat shock element; HSVTK: Minimal herpes simplex virus thymidine kinase promoter; MLuc: *Metridia* luciferase; NP: Nanoparticle; pHSE: Plasmid containing heat shock element sequence; RLU: Relative light units.

that temperature (i.e., thermal dose). Therefore the response of the reporter was measured at various temperature and time combinations. As above, cells were transfected with the HSE–MLuc reporter plasmid and equally divided into three subgroups with five replicates each. Each subgroup was heated by water bath at three different temperatures, 41, 43 and 45°C, for 0–60 min. The temperature of each sample was measured during treatment using calibrated fiber-optic probes (Figure 3A). After heating, cells were transferred to multiwell plates and the secreted MLuc activity measured in fresh cellular media 24 h postexposure (or heating). The resulting thermal-induced reporter activity is displayed as fold RLU, representing the fold HSE signal of each sample relative to a control nonheated sample. A direct response of reporter induction with the treatment temperature and time of treatment was observed (Figure 3B). For studies at 41 and 43°C, the reporter response was linear with treatment time ($R^2 > 0.95$). The reporter response at 45°C was nonlinear and reflective of a Gompertz curve, potentially due to pending heat-induced cell death, which was observed for treatment times longer than 12 min (data not shown). Within this study, no significant cell death was observed among heated samples (Figure 3C).

Thermal dose is conventionally defined by the 'thermal isoeffective dose' or cumulative equivalent minutes (CEM). The canonical equation for thermal dose was derived from studies of cell survival following treatment with a range of temperatures and time [9]. We calculated CEM for all treatment temperatures and found that, for two sublethal treatment doses of 41 and 43°C, reporter activity was a linear function of the CEM for each temperature (Figure 3D). However, the relationship of reporter activity with CEM was dependent on the treatment temperature. For example, reporter signal (fold RLU) and thermal dose (CEM_{43}) at one temperature (41°C) did not always correlate with the expected reporter signal and thermal dose (CEM_{43}) of a sample treated at a different temperature (43°C). This indicates that the end point of HSE reporter activity, as defined by this assay, does not correlate with classically defined thermal dose as defined by the end point of cellular survival. The reporter activity may be similar with other transient cellular responses to mild hyperthermia, which do not result in changes in cell survival [10,12,30,31].

To further characterize reporter response to thermal dose, a separate experiment was performed where the time of cellular treatment was kept constant at 20 min and the temperatures were varied from 37 to 44°C. Specifically, HCT-116 cells were transiently transfected with the HSE–MLuc reporter and then equally divided for treatment over 11 temperatures using a temperature

gradient generated on a PCR heat block. This method allowed multiple temperatures to be simultaneously generated and tested in a single assay. The results confirm that the fold of reporter induction (measured as a ratio of reporter activity from exposed samples relative to controls) is a function of temperature, and demonstrates a linear response within the temperature range of 40–44°C (Figure 4A). The majority of the cells remained viable during this study and only mild cell death could be detected at higher temperatures (Figure 4C). Notably, an approximate 3° rise above physiologic temperature (37°C) was required to produce a statistically significant reporter signal. Statistical analysis using Joinpoint regression software [32] (National Cancer Institute, MD, USA) identified the inflection temperature as 40°C, indicating that heat shock-induced cellular response likely begins at approximately 40°C. This value is similar to that observed by Krawczyk and colleagues [12]. It is notable that the fold signal induced by the heat block at some temperatures differs from that of water bath heating. This may be due to differences in sample volume between the two assays, sample tube thickness, or heat transfer and equilibration between heat block and water bath models.

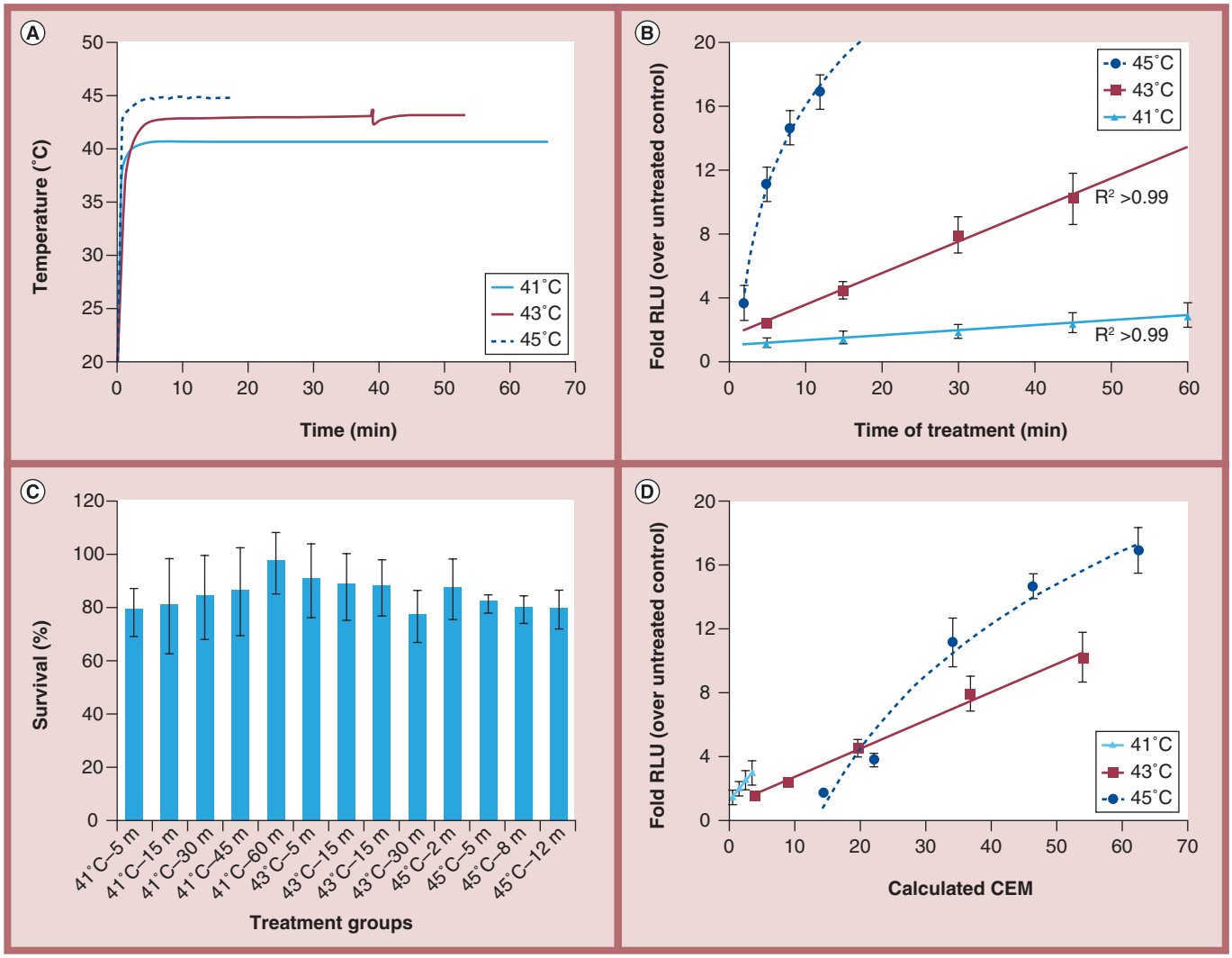

Figure 3. Effect of macroscopic hyperthermia on the reporter. A single population of heat shock element–*Metridia* luciferase (MLuc)-transfected cells was divided and treated at three different temperatures (41, 43 and 45°C) by water bath for 0–60 min. **(A)** The temperature of the cell pellets during the macroscopic water bath-mediated hyperthermia as recorded using FISO systems (FISO Technologies, Quebec City, Canada). **(B)** The corresponding MLuc activity measured 24 h post-treatment. Data are plotted as the fold RLU over the untreated control. **(C)** Cell-viability measurement by MTS assay for the different groups after the MLuc assay. **(D)** Thermal dosimetry and the corresponding MLuc signal. The CEM was calculated by measuring the temperature of the cell pellets with FISO coils using the formula CEM_{43} = Time × $2^{(T-43)}$ for T < 43°C and CEM_{43} = Time × $4^{(T-43)}$ for T > 43°C and plotted against the MLuc signal. Error bars represent standard deviation of four independent measurements.
CEM: Cumulative equivalent minutes; RLU: Relative light units.

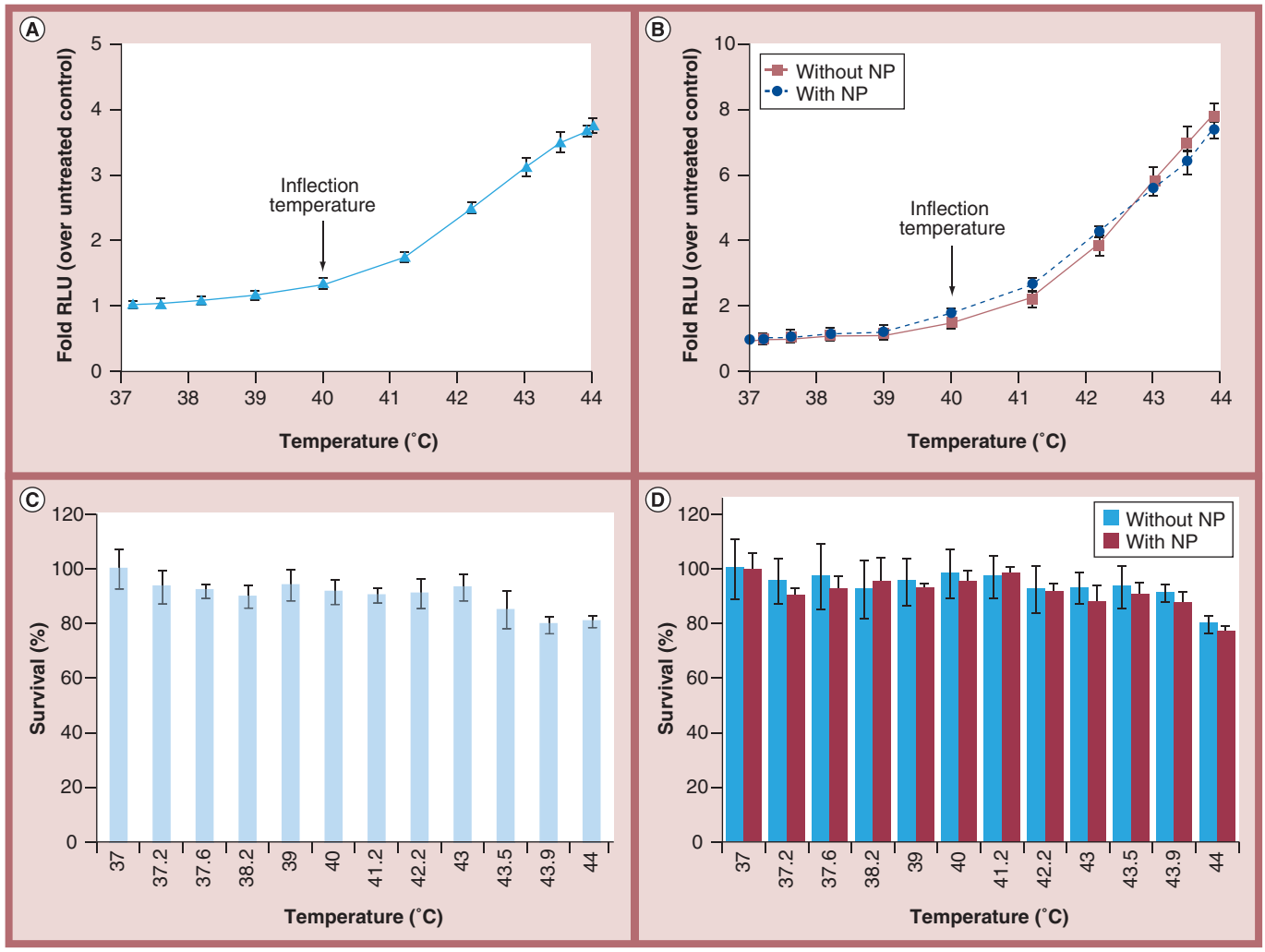

Figure 4. Temperature sensitivity and effect of intracellular nanoparticle on the reporter activity. **(A)** A single population of heat shock element–*Metridia* luciferase (MLuc)-transfected cells were divided and heated at different temperatures for 20 min by heat block (or kept untreated). MLuc signals were measured 24 h post-treatment. Data are plotted as the fold RLU over the untreated control, providing a signal-to-noise ratio. Error bars represent the standard deviation of the mean of four independent measurements. The arrow indicates the inflection temperature as calculated by Joinpoint regression analysis. **(B)** A separate population of heat shock element–MLuc transfected cells were divided and a portion were loaded with bionized nanoferrite NP, while another portion remained nonloaded cells. All cells were then heated at different temperature by heat block for 30 min and MLuc signal plotted against treatment temperature. The arrow indicates the inflection temperature as calculated by Joinpoint regression analysis. **(C)** Displays the corresponding cell viability data as measured by MTS after the MLuc assay for the experiments represented above in **(A)**. **(D)** Displays the corresponding cell viability data as measured by MTS after the MLuc assay for the experiments represented above in **(B)**. Error bars represent standard deviation of four independent measurements.
NP: Nanoparticle; RLU: Relative light units.

A second set of studies was performed to evaluate reporter activity in several other cell models using the same heat block method. Temperature-dependent MLuc reporter activity was observed in all cell lines studied (Supplementary Figure 1). Analysis was performed to identify the inflection point for signal activation for each cell line, as described above. The results found inflection points of 40°C for DU-145 prostate cancer cells, 40°C for MDA-MB-231 breast cancer cells and 41°C for PC-3 prostate cancer cells (Supplementary Figure 1). Taken together, these data indicate that macroscopic hyperthermia induces detectable heat stress at approximately 40–41°C. This is consistent with other reports [30,33,34].

Cellular NP has no effect on the functionality of the sensor

The primary objective of these studies is to evaluate cellular responses to sublethal NP-mediated (nanoscopic) hyperthermia with high sensitivity. It was therefore important to determine whether the NPs would interfere with the sensitivity or linearity of the assay. To investigate this, HCT-116 reporter cells were either

loaded with high concentrations of 100-nm iron oxide NP [35], through the use of poly-D-lysine, as previously reported, or they remained unloaded. The two cell populations (cells with and without NP loading) were then heated to 11 temperatures using the temperature gradient PCR heat block for 30 min. The presence of magnetic iron oxide NPs had no measurable effect on the reporter activity (Figure 4B). The additional 10 min of heating in this second experiment did result in higher reporter activity, as expected. The viability of cells for this second study are reported in Figure 4D.

Monitoring nanoparticle-mediated heating with the biologic sensor

Sensor measures NP-mediated hyperthermia

Having characterized the response of the reporter to macroscopic heating in the presence and absence of NPs, the HSE–MLuc reporter assay was then applied to NP-mediated heating studies with an AMF. An established NP hyperthermia model, utilizing iron oxide NPs and an external AMF, was applied. [27] A single population of cancer cells was transfected with HSE–MLuc reporter vector, as described above, and equally partitioned into treatment groups to be loaded with varying amounts of 100-nm BNF iron-oxide NPs (Supplementary Table 1). Treatment groups were termed 'L0' to 'L4' to indicate increasing levels of NP concentration within the cells, beginning with control cells lacking NPs (L0) to cells loaded with approximately 200 µg of iron oxide NPs. The final concentration of iron oxide NP for each of these treatment groups was measured by ICP-MS and is represented in Table 1. After washing the cells to remove noncell-associated NP, the cells were pelleted and treated in parallel for 20 min by exposure to AMF having a frequency of 150 ± 1 kHz (80 kA/m). For each NP-loaded group, there was a paired control, handled in parallel, which did not receive AMF treatment. A separate 'spike' sample was also included in which NPs were simply mixed with the cells, rather than loaded into the cells, before AMF treatment. After treatment, the NP in the spike sample was removed by cell pelleting and media exchange, in order to prevent any NP-mediated interference in the luciferase assay. The temperature of each sample was measured throughout the treatment by fiber-optic temperature probes (FISO Technologies) placed immediately on the surface of the cell pellet. The total thermal dose of each treatment was measured during the treatment and cool down period, and the calculated T_{mean}, T_{median}, T_{max}, integrated area under the curve and CEM for each cohort are summarized in Table 1. The treatment resulted in different responses. In some samples, such as L1 and L2, measurable macroscopic heating was not achieved (T_{max} < 40°C) (Figure 5A). In other samples, such as L3 and L4, the system was heated to over 40°C (Figure 5B).

Following AMF treatment, the cells were immediately transferred to 96-well plates, fed with fresh media and reporter activity was measured 24 h later. Cell survival was also evaluated by MTS assay (Supplementary Figure 2). HSE–MLuc reporter activity was reported as fold AMF-induced signal (relative to the non-AMF-treated cohort) for each group. As evident from Figure 5C & 5D, statistically significant AMF-induced increase in luciferase expression was observed in all NP-loaded samples (L1 to L4 and spike) when compared with non-NP loaded cells (L0).

NPs can exert hyperthermia effect without a measurable change in temperature

The two samples with the lowest level of loaded iron, L1 and L2, did not induce a measurable temperature change above the previously determined inflection limit of 40°C (Figure 5A & Table 1). Nonetheless, statistically significant reporter induction was observed in these samples where the maximum measured temperatures of only 37.4 and 38.3°C were detected (Figure 5C & Table 1). The calculated CEM of these samples was negligible, with L1 having an identical CEM to the control cells without NP (L0). The higher CEMs were observed in samples L3–L4, which were heated to

Table 1. Dose response of nanoparticle heating.

Group	pg Fe/cell	T_{mean} (°C)	T_{median} (°C)	T_{max} (°C)	AUC	CEM
L0	0.3	36.4	36.4	37.7	48023.2	0.3
L1	37.6	36.6	36.6	38.3	48326.1	0.3
L2	75.2	36.9	36.8	37.4	48797.8	0.4
L3	100.9	39.9	40.5	42.8	52875.8	6.4
L4	255.7	39.5	40.1	41.7	52425.6	3.8
Spike	27.9	40.6	41.2	42.9	53834.7	8.3

Various amounts of nanoparticles were loaded (according to Supplementary Table 1) into HCT-116 cells.
pg Fe/cell indicates iron content quantified by inductively coupled plasma mass spectroscopy.
T_{mean}, T_{median} and T_{max} indicate the mean, median and maximum temperature of the cell pellet measured during the alternating magnetic field treatment and the cool down period.
The AUC and the CEM values are indicative of the total thermal dose for the treatment group.
AUC: Area under the curve; CEM: Cumulative equivalent minutes.

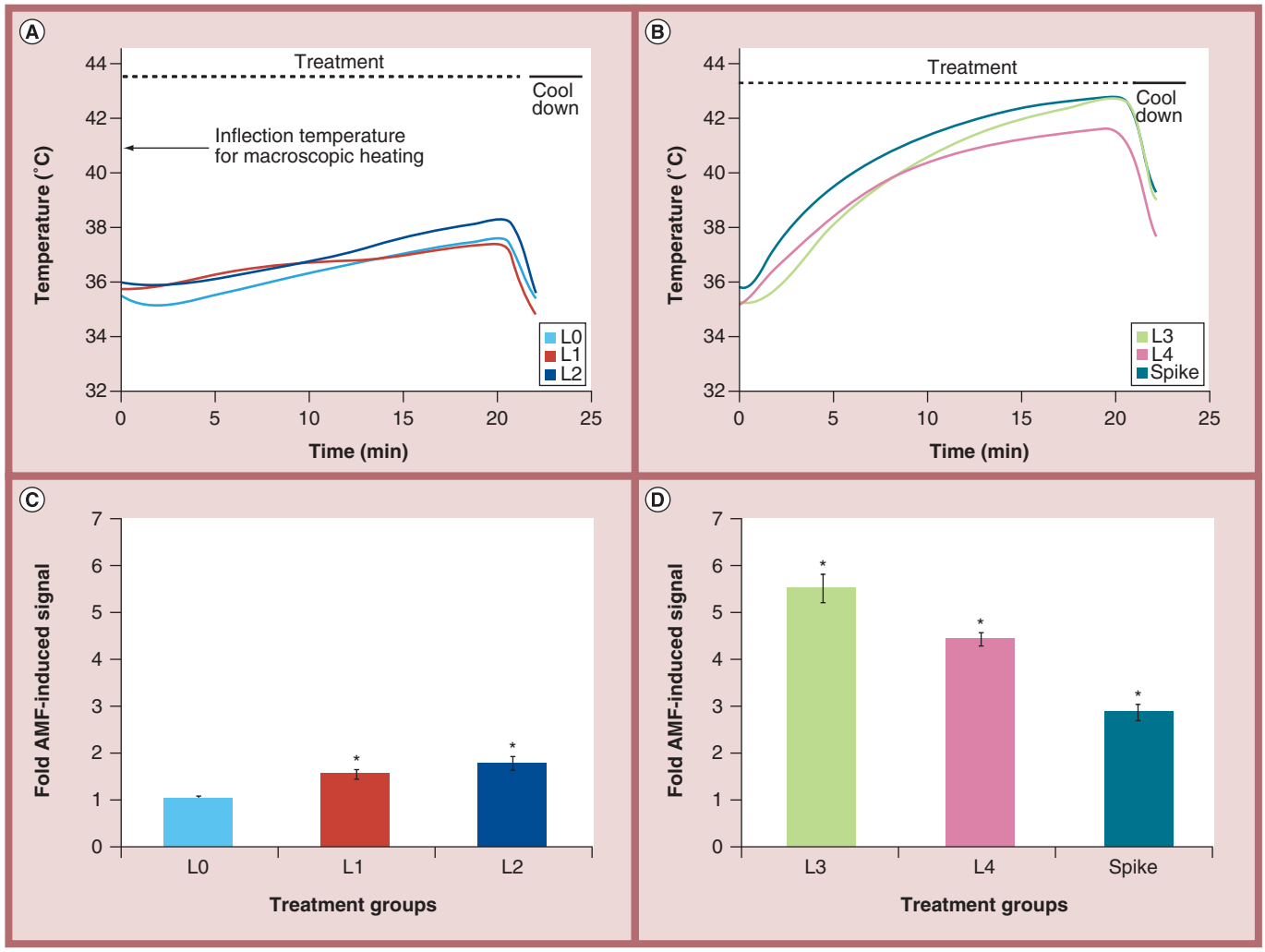

Figure 5. Reporter response to dose-escalated nanoparticle-mediated heating. A single population of heat shock element–*Metridia* luciferase-transfected cells were loaded with various levels of bionized nanoferrite nanoparticle or spiked with external bionized nanoferrite nanoparticle as summarized in Table 1. Each group was divided and half of the cells were heated by exposure to AMF treatment at 80 kA/m for 20 min, while the other half remained nonheated. The temperature of cell pellets during AMF treatment and cool down period were recorded using optical fiber probes. **(A)** Temperature curves of sample L0–L2, which were heated to temperatures below the 40°C inflection points as determined by macroscopic heating. **(B)** Temperature curves of samples L3–L4 and spike, which were heated above the 40°C inflection points as determined by macroscopic heating. **(C)** Fold AMF-induced heat shock element–*Metridia* luciferase signal for samples L0–L2. **(D)** Fold AMF-induced signal for samples L3–L4 and spike. *Statistical significance ($p < 0.001$) compared with the matched untreated-control by Student t-test. Error bars represent the standard deviation of the mean of eight independent measurements.
AMF: Alternating magnetic field.

above 40°C, and where the fold reporter induction was significantly greater (Figure 5D). While sample L3 was loaded with less iron than sample L4, it reached a much higher than anticipated temperature. This difference in temperature between L3 and L4 resulted in a higher reporter signal from L3 when compared with L4, consistent with macroscopic heating. On the other hand, the increased reporter signal measured for samples L1 and L2, which were heated with NPs to temperatures below the 40°C inflection determined with macroscopic heating, provide support that intracellular NP-mediated heating can produce measurable changes to biological processes under very mild thermal conditions that are not observed in macroscopic water bath heating.

The final study group, spike, generated the highest measured thermal dose as calculated by T_{mean}, T_{median}, T_{max}, area under the curve and CEM (Figure 5B & Table 1). Despite this, the corresponding HSE–MLuc reporter activity was considerably lower than the comparably heated L3 sample (Figure 5D). We hypothesize that this may reflect potential differences in cellular response to heating by internalized NPs versus heating by NPs residing outside of the cell. However, we must also consider that the signal may have been influenced by mac-

roscopic heating differences between intracellular and extracellular NPs as measured by temperature on the surface of the cell pellet. Trace amounts of NP may also remain associated with the cells after heating and then possibly resided in the cell growth media and MLuc assay. Additional experiments are therefore required to challenge this hypothesis, which will be addressed in separate studies.

Cell-dilution model to study the relationship of NP-proximity heating to cell stress

It is notable that iron oxide NPs have the potential to produce oxidative cellular stress, by generating hydroxyl free radicals through the Fenton reaction [36,37]. However, as described earlier, no differential reporter activity was observed in NP-loaded versus control cells at these temperatures in macroscopic heating experiments (Figure 4B). To further ensure that the measured reporter activity from NP-loaded cells was related to heating, we conducted an experiment using a cell mixing and dilution model where the NP and reporter were loaded into separate cell populations. With this model, we could also investigate the effect of NP proximity heating on cellular thermal stress. The maximum temperatures of the cell pellet in these studies were intentionally limited to below 40°C to limit potential for macroscopic heating to affect the response of the entire population of cells. Specifically, three treatment cohorts were generated with a fixed number of iron oxide NP-loaded 'heater cells' (750,000 cells), which were loaded under conditions identical to L4 (Supplementary Table 1), and an increasing density of HSE–MLuc transfected 'reporter cells'. Thus, the reporter cells do not contain NPs and can only measure thermal stress generated from neighboring NP-loaded cells. The total cell number for each treatment cohort was fixed at 1.5 million cells by adding nontransfected 'filler cells'. This model generated low, medium and high ratios (Low-R, Med-R and Hi-R) of reporter cells to NP-loaded heater cells. The three different mixtures were then subjected to identical AMF hyperthermia conditions in parallel, with matching samples that remained unexposed to AMF treatment. The temperature of the cell pellet and the MLuc reporter activity were recorded for each sample as described above and reported as fold AMF-induced signal. The temperature profile was similar for all three mixtures, none of which reached a mean temperature above 37°C (Figure 6A & Supplementary Figure 3). Notably, the fold-induced reporter response was proportional to the ratio of reporter to heater cells (Figure 6B). This suggests that when reporter cells are closer to heater cells (i.e., Hi-R vs Low-R), they receive greater thermal stress. Furthermore, because the NPs are not within the reporter cells, the stress should not be due to NP association with intracellular structures. There was no statistically significant difference between the groups with medium (Med-R) and high (Hi-R) reporter density, indicating that the proximity of the heater and reporter cells was not sufficiently different between these two groups. Taken together, the results of Figures 5 & 6 suggest that NP-mediated hyperthermia, under conditions in which the temperature of the system is not measurably affected, can have local effects. This model provides a new way to compare response to NP versus macroscopic heating in living cells.

Discussion

Here we have developed and applied a temperature-sensitive reporter plasmid that uses a secreted bioluminescent reporter to compare cellular responses to macroscopic and NP-mediated (nanoscopic) hyperthermia. The reporter is expressed at high levels by a constitutively active herpes simplex virus thymidine kinase minimal promoter that is made heat responsive through a HSE enhancer. Upon heat shock, the HSF-1 transcription factor is activated to bind the HSE and to further activate MLuc reporter transcription. Thermally induced MLuc activity was detected between 4 and 24 h after heat shock (Figure 2), but could possibly remain active for longer periods of time before recovering to a native state. The thermally induced signal, conveyed as fold RLU relative to nonheated cells, is responsive over a range of nonlethal temperatures from 40 to 45°C. The resulting biosensor has some advantages over previously reported thermal sensors. The high-sensitivity MLuc assay can be applied to small sample volumes and is linear over a multilog dynamic range [24]. The cost of the assay is also minimal and requires only coelenterazine and oxygen. It therefore has the potential to be applied to high-throughput screens, such as for NP potency or heating efficiency. The signal is also a measurement of relative cellular response to thermal stress, rather than only to temperature. Thus the assay provides a different perspective than thermally responsive probes. Finally, the use of a secreted reporter provides the advantage of separating the reporter measurement from the cellular and NP components, which may influence detection through spectral absorbance or assay inhibition. The remaining cells can then be studied for alternative biologic responses, such as viability.

The described assay also has limitations that should be considered. Notably, the assay requires viable cells for activity. Therefore, the assay is limited to mild hyperthermic conditions that induce minimal cell death. Alternative thermal assays should be considered for thermally ablative or highly cytotoxic conditions. Another potential limitation of the assay is the influence of cellular transfection efficiency on reporter activity. To address

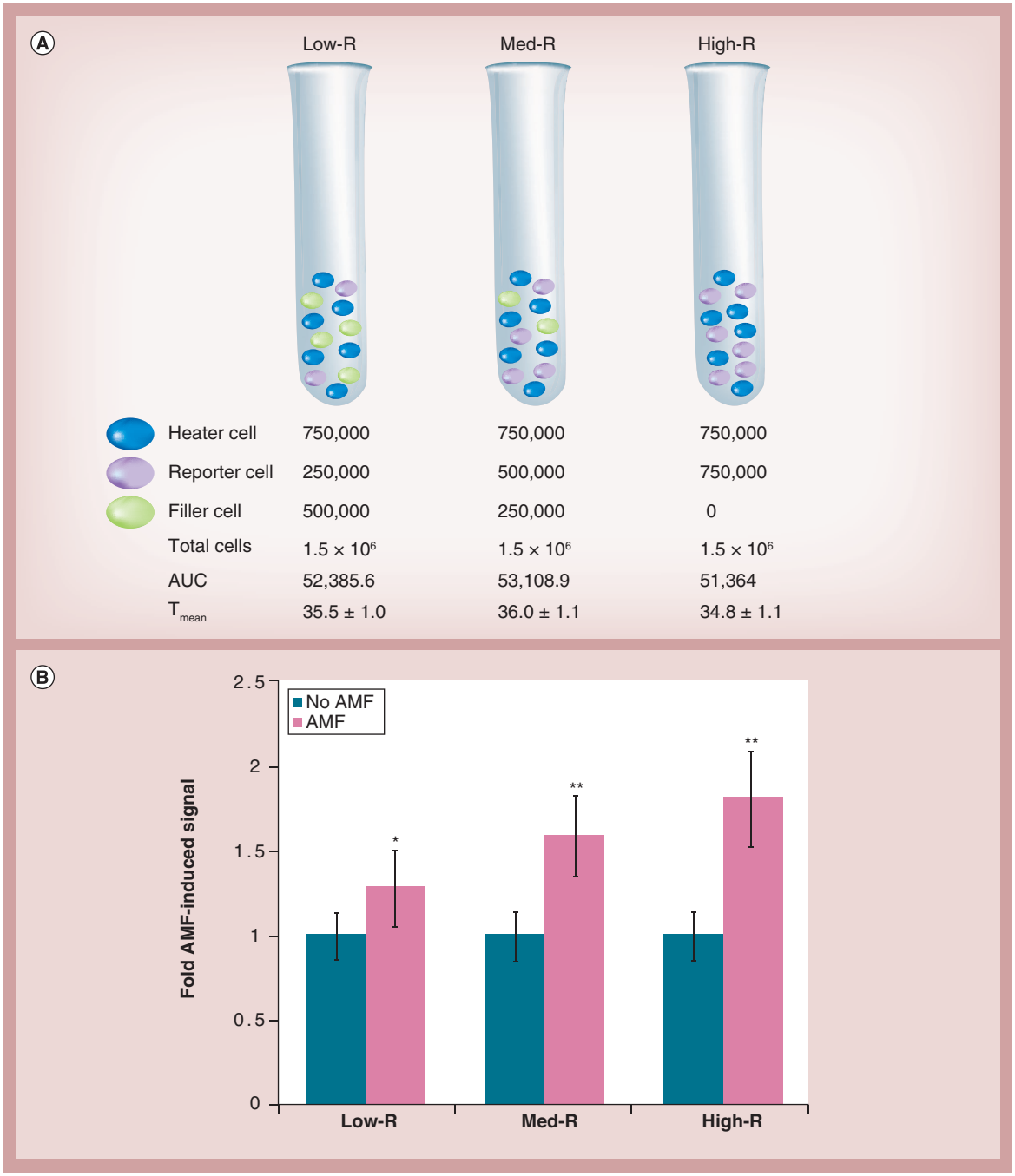

Figure 6. Evaluation of cellular response to different ratios of nanoparticle-mediated cell heating. (A) Schematic of experimental design in which a fixed amount of nanoparticle-loaded 'heater cells' are mixed with varying amounts of heat shock element reporter-loaded 'reporter cells' to generate Low-R, Med-R and Hi-R with respect to heater cells. To maintain a constant system size of 1.5 million total cells, 'filler cells', the number of cells, mean temperature (°C), and thermal dose (calculated as AUC) of the cell pellet is indicated for each treatment condition. Each of the three mixtures were halved and exposed, or not exposed, to identical AMF treatment and then transferred to multiwell plates for heat shock element–*Metridia* luciferase reporter analysis. **(B)** Reporter cell response correlates with the density of nanoparticle-loaded cell heating. Data are plotted as the fold AMF-induced signal. The data are an average of four independent experiments performed on different days. *Statistical significance: $p < 0.01$; **statistical significance: $p < 0.001$, compared with the matched untreated-control by Student t-test. Error bars represent the standard deviation of the mean of eight independent measurements.
AMF: Alternating magnetic field; AUC: Area under the curve; Hi-R: High density of reporter cells; Low-R: Low density of reporter cells; Med-R: Medium density of reporter cells.

this, we performed each study with a single transfected population that was then partitioned into separate treatment groups, and all data were then reported as relative or fold-induced signal. If one wishes to compare multiple different populations or independent assays, the results should be normalized for transfection efficiency. It is important to note that the assay, in the present form, cannot be used as a thermometer or dosimeter to measure absolute or objective temperatures, thermal dose or NP dose. It is, rather, an effective measure of relative cell stress response to stimuli (e.g., heat) when appropriately calibrated against controls. This is because the rate of reporter activity can vary with different systemic temperatures (Figure 3D). One should also consider that the assay may respond differently with repeated treatments or cellular thermotolerance, which was not evaluated in these studies. Finally, the complexity of cellular signaling and heat shock response should be considered for each experiment. Cellular stress and toxicity can be activated by multiple stimuli. For example, Asin and colleagues recently reported that media from cells heated with magnetic NPs was nearly 100% toxic to a nonheated cell population [38], indicating that a toxic signal was released from the heated cells. It is unlikely that a similar pathway was responsible for the reporter activity observed in these studies, because little to no cell death was observed from the mild hyperthermia applied (Supplementary Figures 2 & 4), nor was measurable reporter activity noted in appropriate control samples. The results also indicate that the NPs had no influence on reporter activity in the presence or absence of heat (Figures 4B & 5). Nonetheless, one must consider that other cellular signaling pathways or cytotoxic activities may influence reporter activity.

The reported assay is functional and linear in the range of mild hyperthermia (40–43°C). This is a clinically relevant temperature range for hyperthermia as it makes the cells more susceptible to radiation or chemotherapy, as recently emphasized by Krawczyk *et al.* [12]. The assay may therefore have an application in predicting cellular response to combination therapies using very mild hyperthermia. For example, the assay was capable of detecting cellular stress at very lose doses of hyperthermia (CEM: 0.3–8.3; Table 1). We believe that this sensitivity allowed us to detect a unique form of thermal stress from neighboring cells under submacroscopic heating conditions (Figure 6). In addition, the assay revealed another interesting phenomenon regarding the rate of sublethal thermal stress. Specifically, cells treated with lower treatment temperatures (41°C) displayed a steeper activation slope over time when compared with higher treatment temperatures (43°C) (Figure 3D). This may indicate different biological responses to different sublethal temperatures. Cumulatively, these results, as well as previous studies of cellular stress under mild and nonlethal hyperthermic conditions [13,16], may reveal a new realm of thermal dosing that is active below the applicable range of CEM calculation, which is based on cell death. Recent reports have revealed that mild hyperthermia (<43°C) produces rich and complex responses in cells affecting their ability to respond to other stresses resulting from clinically relevant sources such as ionizing radiation. Further studies in this realm of mild hyperthermia are needed to characterize and quantify these phenomena because they present new and exciting directions for clinical application.

Conclusion

We report the development and application of a temperature-sensitive biologic sensor system to investigate cellular response to NP heating. The secreted reporter signal was found to be a direct function of the temperature of the system and the time at temperature. The assay system was capable of measuring cellular response to both macroscopic and NP-mediated hyperthermia. With NP-mediated hyperthermia, cellular stress could be detected under conditions where there were no measurable differences in the temperature of the system. This cellular stress was detectable when the NPs were loaded into reporter cells or when the NPs were in adjacent cells. Cell dilution experiments suggest that the proximity of cells to NP heating can influence the biologic response. Collectively these studies indicate that NP hyperthermia may produce a different kind of cellular response when compared with macroscopic heating. Additional cell-based reporter systems and studies may offer insights and new information to elucidate mechanisms of cellular response to NP-based hyperthermia.

Future perspective

Understanding the consequences of heat transfer in cells is important for NP-mediated hyperthermia because clinical translation depends upon the ability of relatively small numbers of NPs to influence sizeable and complex tissues. Intracellular biological sensors that produce quantifiable signal with related cell stress, can be used to understand how NP-mediated hyperthermia may differ from macroscopic hyperthermia. The results of these studies indicate that mild or even unmeasurable NP-mediated hyperthermia can activate cellular stress pathways. In light of this, we hypothesize that very mild doses of NP-mediated hyperthermia may be detected by this assay and used to provide information for combinations with other therapies. The results of this study suggest that the proximity of cells to NP heating can also influence the cellular stress response. Therefore, differences in NP administration or distribution may result in distinct therapeutic responses. These phenom-

ena may not be unique to iron oxide NPs or NP-mediated hyperthermia. It would be valuable to study cellular stress response with other nanomaterials and nanotherapeutics, both intracellularly and extracellularly, under mild hyperthermic conditions.

Disclaimer

The content is solely the responsibility of the authors and does not necessarily represent the official views of the National Cancer Institute or the NIH.

Acknowledgements

The authors thank WH Chowdhury, D Coffey and L Chung for their valuable suggestions and critical discussions regarding this work. They also thank A Attaluri, M Seshadri and S Budri for their technical assistance.

Financial & competing interests disclosure

Funding for this project was supported by a grant from the Safeway Foundation and the Prostate Cancer Foundation (TL DeWeese and RH Getzenberg), a gift from the Mr. David Koch Foundation (SEL), and by Award Number U54CA143803 from the National Cancer Institute (R Ivkov). Inductively coupled plasma mass spectroscopy analysis was supported in part by the Maryland Cigarette Restitution Fund Program at the Johns Hopkins Bloomberg School of Public Health and the NIEHS Center P30E00319. The authors have no other relevant affiliations or financial involvement with any organization or entity with a financial interest in or financial conflict with the subject matter or materials discussed in the manuscript apart from those disclosed.

No writing assistance was utilized in the production of this manuscript.

Executive summary

Objective

- To develop and apply a temperature-sensitive secreted luciferase-based reporter gene system to study thermal stress response, at the cellular level, to macroscopic and nanoparticle (NP) hyperthermia.

Materials & methods

- A heat-responsive reporter applying the heat shock element and a constitutively active secreted *Metridia* luciferase reporter.
- Water bath and heat blocks were used as sources of macroscopic heating.
- 100-nm commercially available iron oxide nanoparticles and an alternating magnetic field system were used to generate nanoscopic heating.
- HCT-116 colon cancer cells were used as a model cell line.

Results & discussion

- In macroscopic heating, the reporter signal was found to be a direct function of temperature and time at temperature.
- NP-mediated hyperthermia can induce cellular stress at doses too low to measurably change the temperature of the system.
- NP-mediated hyperthermia can induce measurable heat response in neighboring cells.
- The stress a cell perceives from NP-mediated hyperthermia can be a function of proximity to NP heating.

Conclusion

- NP-mediated hyperthermia perturbs the cellular machinery in a distinct way. The presently described biological sensor can be used to explore more details about the nanoscopic mode of hyperthermia.

References

Papers of special note have been highlighted as:
◦ of interest

1 Ahmed N, Fessi H, Elaissari A. Theranostic applications of nanoparticles in cancer. *Drug Discov. Today* 17, 928–934 (2012).

• Chatterjee DK, Diagaradjane P, Krishnan S. Nanoparticle-mediated hyperthermia in cancer therapy. *Ther. Deliv.* 2(8), 1001–1014 (2011).

2 Nielsen OS, Horsman M, Overgaard J. A future for hyperthermia in cancer treatment? *Eur. J. Cancer* 37(13), 1587–1589 (2001).

3 Gordon RT, Hines JR, Gordon D. Intracellular hyperthermia. A biophysical approach to cancer treatment via intracellular temperature and biophysical alterations. *Med. Hypotheses* 5(1), 83–102 (1979).

4 Basel MT, Balivada S, Wang H *et al.* Cell-delivered magnetic nanoparticles caused hyperthermia-mediated increased survival in a murine pancreatic cancer model. *Int. J. Nanomedicine* 7, 297–306 (2012).

5 Giustini AJ, Ivkov R, Hoopes PJ. Magnetic nanoparticle biodistribution following intratumoral administration. *Nanotechnology* 22(34), 345101 (2011).

6 Johannsen M, Gneveckow U, Thiesen B *et al.* Thermotherapy of prostate cancer using magnetic nanoparticles: feasibility, imaging, and three-dimensional temperature distribution. *Eur. Urol.* 52(6), 1653–1661 (2007).

7 Maier-Hauff K, Ulrich F, Nestler D *et al.* Efficacy and safety of intratumoral thermotherapy using magnetic iron-oxide nanoparticles combined with external beam radiotherapy on patients with recurrent glioblastoma multiforme. *J. Neurooncol.* 103(2), 317–324 (2011).

8 Dewey WC. Arrhenius relationships from the molecule and cell to the clinic. *Int. J. Hyperthermia* 25(1), 3–20 (2009).

9 Kariya A, Tabuchi Y, Yunoki T, Kondo T. Identification of common gene networks responsive to mild hyperthermia in human cancer cells. *Int. J. Mol. Med.* 32(1), 195–202 (2013).

10 Roti Roti JL. Cellular responses to hyperthermia (40–46°C): cell killing and molecular events. *Int. J. Hyperthermia* 24(1), 3–15 (2008).

11 Krawczyk PM, Eppink B, Essers J *et al.* Mild hyperthermia inhibits homologous recombination, induces BRCA2 degradation, and sensitizes cancer cells to poly(ADP-ribose) polymerase-1 inhibition. *Proc. Natl Acad. Sci. USA* 108(24), 9851–9856 (2011).

12 Creixell M, Bohorquez AC, Torres-Lugo M, Rinaldi C. EGFR-targeted magnetic nanoparticle heaters kill cancer cells without a perceptible temperature rise. *ACS Nano* 5(9), 7124–7129 (2011).

- **Demonstrates that iron oxide nanoparticles (NP) can kill cells without temperature rise.**

13 Asin L, Ibarra MR, Tres A, Goya GF. Controlled cell death by magnetic hyperthermia: effects of exposure time, field amplitude, and nanoparticle concentration. *Pharm. Res.* 29(5), 1319–1327 (2012).

14 Villanueva A, De La Presa P, Alonso JM *et al.* Hyperthermia HeLa cell Treatment with silica-coated manganese oxide nanoparticles. *J. Phys. Chem. C* 114(5), 1976–1981 (2010).

15 Krpetic Z, Nativo P, See V, Prior IA, Brust M, Volk M. Inflicting controlled nonthermal damage to subcellular structures by laser-activated gold nanoparticles. *Nano Lett.* 10(11), 4549–4554 (2010).

16 Jordan A, Scholz R, Wust P *et al.* Endocytosis of dextran and silan-coated magnetite nanoparticles and the effect of intracellular hyperthermia on human mammary carcinoma cells *in vitro*. *J. Magnet. Magn. Mater.* 194(1–3), 185–196 (1999).

17 Rodriguez-Luccioni HL, Latorre-Esteves M, Mendez-Vega J *et al.* Enhanced reduction in cell viability by hyperthermia induced by magnetic nanoparticles. *Int. J. Nanomedicine* 6, 373–380 (2011).

18 Gota C, Okabe K, Funatsu T, Harada Y, Uchiyama S. Hydrophilic fluorescent nanogel thermometer for intracellular thermometry. *J. Am. Chem. Soc.* 131(8), 2766–2767 (2009).

19 Huang H, Delikanli S, Zeng H, Ferkey DM, Pralle A. Remote control of ion channels and neurons through magnetic-field heating of nanoparticles. *Nat. Nanotechnol.* 5(8), 602–606 (2010).

20 Yang JM, Yang H, Lin L. Quantum dot nano thermometers reveal heterogeneous local thermogenesis in living cells. *ACS Nano* 5(6), 5067–5071 (2011).

21 Raoof M, Zhu C, Kaluarachchi WD, Curley SA. Luciferase-based protein denaturation assay for quantification of radiofrequency field-induced targeted hyperthermia: Developing an intracellular thermometer. *Int. J. Hyperthermia* 28(3), 202–209 (2012).

- **Uses a denaturation-based luciferase assay to detect macroscopic hyperthermia.**

22 Deckers R, Debeissat C, Fortin PY, Moonen CT, Couillaud F. Arrhenius analysis of the relationship between hyperthermia and Hsp70 promoter activation: a comparison between *ex vivo* and *in vivo* data. *Int. J. Hyperthermia* 28(5), 441–450 (2012).

23 Lupold SE, Johnson T, Chowdhury WH, Rodriguez R. A real time *Metridia* luciferase based non-invasive reporter assay of mammalian cell viability and cytotoxicity via the beta-actin promoter and enhancer. *PLoS ONE* 7(5), e36535 (2012).

24 Pelham HR. A regulatory upstream promoter element in the *Drosophila* hsp70 heat-shock gene. *Cell* 30(2), 517–528 (1982).

25 Wu BJ, Kingston RE, Morimoto RI. Human HSP70 promoter contains at least two distinct regulatory domains. *Proc. Natl Acad. Sci. USA* 83(3), 629–633 (1986).

26 Hedayati M, Thomas O, Abubaker-Sharif B *et al.* The effect of cell-cluster size on intracellular nanoparticle-mediated hyperthermia: is it possible to treat microscopic tumors? *Nanomedicine (Lond.)* 8, 29–41 (2012).

- **Very elegant paper that used similar NP-loaded cell cluster model.**

27 Bordelon DE, Cornejo C, Gruettner C, Westphal F, Deweese TL, Ivkov R. Magnetic nanoparticle heating efficiency reveals magneto-structural differences when characterized with wide ranging and high amplitude alternating magnetic fields. *J. Appl. Phys.* 109(12), 124904 (2011).

28 Joinpoint Regression Program. http://surveillance.cancer.gov/joinpoint

29 Di YP, Repasky EA, Subjeck JR. Distribution of HSP70, protein kinase C, and spectrin is altered in lymphocytes during a fever-like hyperthermia exposure. *J. Cell Physiol.* 172(1), 44–54 (1997).

30 Park HG, Han SI, Oh SY, Kang HS. Cellular responses to mild heat stress. *Cell. Mol. Life Sci.* 62(1), 10–23 (2005).

31 Kim HJ, Fay MP, Feuer EJ, Midthune DN. Permutation tests for joinpoint regression with applications to cancer rates. *Stat. Med.* 19(3), 335–351 (2000).

32 Field SB, Morris CC. The relationship between heating time and temperature: its relevance to clinical hyperthermia. *Radiother. Oncol.* 1(2), 179–186 (1983).

33 Overgaard J, Suit HD. Time-temperature relationship th hyperthermic treatment of malignant and normal tissue *in vivo*. *Cancer Res.* 39(8), 3248–3253 (1979).

34 Gruettner C, Mueller K, Teller J, Westphal F, Foreman A, Ivkov R. Synthesis and antibody conjugation of magnetic nanoparticles with improved specific power absorption rates for alternating magnetic field cancer therapy. *J. Magnet. Magn. Mater.* 311(1), 181–186 (2007).

- **Describes synthesis and properties of iron oxide NP used in the present manuscript.**

35 Klein S, Sommer A, Distel LV, Neuhuber W, Kryschi C. Superparamagnetic iron oxide nanoparticles as radiosensitizer via enhanced reactive oxygen species formation. *Biochem. Biophys. Res. Commun.* 425(2), 393–397 (2012).

36 Voinov MA, Sosa Pagan JO, Morrison E, Smirnova TI, Smirnov AIi. Surface-mediated production of hydroxyl radicals as a mechanism of iron oxide nanoparticle biotoxicity. *J. Am. Chem. Soc.* 133(1), 35–41 (2011).

37 Asin L, Goya GF, Tres A, Ibarra MR. Induced cell toxicity originates dendritic cell death following magnetic hyperthermia treatment. *Cell Death Dis.* 4, e596 (2013).